

Effect of strong magnetic field on competing order parameters in two-flavor dense quark matter

Tanumoy Mandal^{1,*} and Prashanth Jaikumar^{2,†}

¹*Department of Physics and Astronomy,
Uppsala University, Box 516, SE-751 20 Uppsala, Sweden*

²*Department of Physics and Astronomy,
California State University Long Beach, Long Beach, CA 90840 USA*

(Dated: March 10, 2022)

Abstract

We study the effect of strong magnetic field on competing chiral and diquark order parameters in a regime of moderately dense quark matter. The inter-dependence of the chiral and diquark condensates through nonperturbative quark mass and strong coupling effects is analyzed in a two-flavor Nambu-Jona-Lasinio (NJL) model. In the weak magnetic field limit, our results agree qualitatively with earlier zero-field studies in the literature that find a critical coupling ratio $G_D/G_S \sim 1.1$ below which chiral or superconducting order parameters appear almost exclusively. Above the critical ratio, there exists a significant mixed broken phase region where both gaps are non-zero. However, a strong magnetic field $B \gtrsim 10^{18}$ G disrupts this mixed broken phase region and changes a smooth crossover found in the weak-field case to a first-order transition for both gaps at almost the same critical density. Our results suggest that in the two-flavor approximation to moderately dense quark matter, strong magnetic field enhances the possibility of a mixed phase at high density, with implications for the structure, energetics and vibrational spectrum of neutron stars.

PACS numbers: 26.60.-c, 24.85.+p, 97.60.Jd

Keywords: quark matter, color superconductivity, neutron stars

*Electronic address: tanumoy.mandal@physics.uu.se

†Electronic address: prashanth.jaikumar@csulb.edu

I. INTRODUCTION

The existence of deconfined quark matter in the dense interior of a neutron star is an interesting question that has spurred research in several new directions in nuclear astrophysics. On the theoretical side, it has been realized that cold and dense quark matter must be in a superconductor/superfluid state [1–6] with many possible intervening phases [7–14] between a few times nuclear matter density to asymptotically high density, where quarks and gluons interact weakly. The observational impact of these phases on neutron star properties can be varied and dramatic [15–22]. Therefore, it is of interest to situate theoretical ideas and advances in our understanding of dense quark matter in the context of neutron stars, which serve as unique astrophysical laboratories for such efforts. The phase structures of hot quark matter have been probed in experiments such as in heavy-ion collisions at the Relativistic Heavy Ion Collider (RHIC) and at the Large Hadron Collider (LHC). It is estimated in Refs. [23–25] that the magnetic field originating from off-central nucleon-nucleon collisions at these colliders can be as large as $10^{18} - 10^{20}$ G. On the astrophysical side, the strength of the magnetic field in some magnetars is of the order $10^{14} - 10^{15}$ G [26], while in the core of such objects, magnetic field might reach up to $10^{18} - 10^{19}$ G. Therefore, it is not surprising that many recent works have stressed the role of strong magnetic fields on hot or dense quark matter [27–35].

At very high density (*i.e.* $\mu \gg \Lambda_{\text{QCD}}$ where μ is the baryon chemical potential and Λ_{QCD} is the scale of quantum chromodynamics) and for number of flavors $N_f = 3$, the preferred pairing pattern is a flavor and color democratic one termed as the color-flavor-locked (CFL) phase [7]. This idealized phase, while it displays the essentially novel features of the color superconducting state, is unlikely to apply to the bulk of the neutron star matter, since even ten times nuclear matter saturation density (ρ_0) only corresponds to a quark chemical potential $\mu \sim 500$ MeV. At these densities, quark mass and strong coupling effects can be important, and must be treated nonperturbatively. It is reasonable to think that the strange quark current mass, being much larger than that of the up and down quarks, inhibits pairing of strange quarks with light quarks. For the purpose of this work, we therefore adopt the scenario of quark matter in the two-flavor superconducting phase, which breaks the color SU(3) symmetry to SU(2), leaving light quarks of one color (say “3”) and all colors of the strange quark unpaired. Although this phase initially

appeared to be disfavored in compact stars [36, 37] once constraints of neutrality were imposed within a perturbative approach to quark masses, the NJL model where masses are treated dynamically still allows for the 2SC phase. Since the issue is not settled, we proceed by adopting the NJL model which best highlights the competition between the chiral and diquark condensates in a straightforward way. Also, our results will be qualitatively true for the 2SC+s phase [9, 10], which can be studied similarly by simply embedding the strange quark, which is inert with respect to pairing, in the enlarged three-flavor space. The additional complications of compact star constraints have been examined before [27, 35, 38], and do not change the main qualitative conclusions of the present work, namely, that strong magnetic field alters the competition between the chiral and diquark order parameters from the weak-field case.

Our objective in this paper is a numerical study of the competition between the chiral and diquark condensates at moderately large μ and large magnetic field using the NJL model, similar in some respects to previous works [8, 9, 39–41], which treat the quark mass non-perturbatively. Instanton-based calculations and random-matrix methods have also been employed in studying the interplay of condensates [42–44]. In essence, smearing of the Fermi surface by diquark pairing can affect the onset of chiral symmetry restoration, which happens at $\mu \sim M_q$, where M_q is the constituent quark mass scale [45]. Since M_q appears also in the (Nambu-Gorkov) quark propagators in the gap equations, a coupled analysis of chiral and diquark condensates is required. This was done for the two-flavor case with a common chemical potential in [8], but for zero magnetic field. We use a self-consistent approach to calculate the condensates from the coupled gap equations, and find small quantitative (but not qualitative) differences from the results of Huang et. al. [8] for zero magnetic field. This small difference is most likely attributed to a difference in numerical procedures in solving the gap equations. We also address the physics of chiral and diquark condensates affected by large in-medium magnetic field that are generated by circulating currents in the core of a neutron or hybrid star. Magnetic field in the interior of neutron stars may be as large as 10^{19} G, pushing the limits of structural stability of the star [46, 47]. There is no Meissner effect for the rotated photon, which has only a small gluonic component, therefore, magnetic flux is hardly screened [48], implying that studies of magnetic effects in color superconductivity are highly relevant. Note that the rotated gluonic field, which has a very small photonic component, is essentially screened due to

the 2SC phase. Including the magnetic interaction of the quarks with the external field leads to qualitatively different features in the competition between the two condensates, and this is the main result of our work.

In Section II, we state the NJL model Lagrangian for the 2SC quark matter. In Section III, we recast the partition function and thermodynamic potential in terms of interpolating bosonic variables. In Section IV, we obtain the gap equations for the chiral and diquark order parameters by minimizing the thermodynamic potential (we work at zero temperature throughout since typical temperature in stars, $T_{\text{star}} \ll \mu$). In Section V, we discuss our numerical results for the coupled evolution of the condensates as functions of a single ratio of couplings, chemical potential and magnetic field before concluding in Section VI.

II. LAGRANGIAN FOR 2SC QUARK MATTER

The Lagrangian density for two quark flavors ($N_f = 2$) applicable to the scalar and pseudoscalar mesons and scalar diquarks is

$$\begin{aligned} \mathcal{L} = & \bar{q} \left[i\gamma^\mu (\partial_\mu - ieQA_\mu - igT^8 G_\mu^8) + \hat{\mu}\gamma^0 - \hat{m} \right] q + G_S \left[(\bar{q}q)^2 + (\bar{q}i\gamma_5 \vec{\tau} q)^2 \right] \\ & + G_D \left[(\bar{q}i\gamma_5 \epsilon_f \epsilon_c q^C) (\bar{q}^C i\gamma_5 \epsilon_f \epsilon_c q) \right] , \end{aligned} \quad (1)$$

where $q \equiv q_{ia}$ is a Dirac spinor which is a doublet (where $i = \{u, d\}$) in flavor space and triplet (where $a = \{1, 2, 3\}$) in color space. The charge-conjugated fields are defined as $\bar{q}^C = -q^T C$ and $q^C = C\bar{q}^T$ with charge-conjugation matrix $C = -i\gamma^0\gamma^2$. The components of the $\vec{\tau} = (\tau^1, \tau^2, \tau^3)$ are the Pauli matrices in flavor space and, $(\epsilon_f)_{ij}$ and $(\epsilon_c)^{\alpha\beta 3}$ are the antisymmetric matrices in flavor and color spaces respectively. The common quark chemical potential is denoted as $\hat{\mu}$ ¹ and $\hat{m} = \text{diag}(m_u, m_d)$ is the current quark mass matrix in the flavor basis. We take the exact isospin symmetry limit, $m_u = m_d = m_0 \neq 0$. The U(1) and SU(3)_c gauge fields are denoted by A_μ and G_μ respectively. Here, e is the electromagnetic charge of an electron and g is the SU(3)_c coupling constant. The electromagnetic charge matrix for quark is defined as $Q = Q_f \otimes \mathbf{1}_c$ with $Q_f \equiv \text{diag}(2/3, -1/3)$

¹ For simplicity we assume a common chemical potential for all quarks. In an actual neutron star containing some fraction of charge neutral 2SC or 2SC+s quark matter in β -equilibrium, additional chemical potentials for electric charge and color charges must be introduced in the NJL model. Furthermore, there can be more than one diquark condensate and in general $M_u \neq M_d \neq M_s$ [9].

(in unit of e). The couplings of the scalar and diquark channels are denoted as G_S and G_D respectively. In general, one can extend the NJL Lagrangian considered in Eq. 1 by including vector and t' Hooft interaction terms which can significantly affect the equation of state of the compact stars with superconducting quark core [49, 50]. In this paper, our main aim is to investigate the competition between chiral and diquark condensates and therefore, we do not consider other interactions in our analysis.

We introduce auxiliary bosonic fields to bosonize the four-fermion interactions in Lagrangian (1) via a Hubbard-Stratonovich (HS) transformation. The bosonic fields are

$$\sigma = (\bar{q}q); \quad \vec{\pi} = (\bar{q}i\gamma_5\vec{\tau}q); \quad \Delta = (\bar{q}^C i\gamma_5\epsilon_f\epsilon_c q); \quad \Delta^* = (\bar{q}i\gamma_5\epsilon_f\epsilon_c q^C); \quad (2)$$

and after the HS transformation, the bosonized Lagrangian density becomes

$$\begin{aligned} \mathcal{L} = & \bar{q} [i\gamma^\mu (\partial_\mu - ieQA_\mu - igT^8 G_\mu^8) + \hat{\mu}\gamma^0] q - \bar{q} (m + i\gamma_5\vec{\pi} \cdot \vec{\tau}) q \\ & - \frac{1}{2}\Delta^* (\bar{q}^C i\gamma_5\epsilon_f\epsilon_c q) - \frac{1}{2}\Delta (\bar{q}i\gamma_5\epsilon_f\epsilon_c q^C) - \frac{\sigma^2 + \vec{\pi}^2}{4G_s} - \frac{\Delta^*\Delta}{4G_D}, \end{aligned} \quad (3)$$

where $m = m_0 + \sigma$. We set $\vec{\pi} = 0$ in our analysis, which excludes the possibility of pion condensation for simplicity [51]. Order parameters for chiral symmetry breaking and color superconductivity in the 2SC phase are represented by non-vanishing vacuum expectation values (VEVs) for σ and Δ . The diquark condensates of u and d quarks carry a net electromagnetic charge, implying that there is a Meissner effect for ordinary magnetism, while a linear combination of the photon and gluon leads to a “rotated” massless U(1) field which is identified as the in-medium photon. We can write the Lagrangian in terms of rotated quantities using the following identity,

$$eQA_\mu + gT^8 G_\mu^8 = \tilde{e}\tilde{Q}\tilde{A}_\mu + \tilde{g}\tilde{T}^8\tilde{G}_\mu^8. \quad (4)$$

In the *r.h.s.* of the Eq. (4) all quantities are rotated. In $flavor \otimes color$ space in units of the rotated charge of an electron $\tilde{e} = \sqrt{3}ge/\sqrt{3g^2 + e^2}$ the rotated charge matrix is

$$\tilde{Q} = Q_f \otimes \mathbf{1}_c - \mathbf{1}_f \otimes \frac{T_c^8}{2\sqrt{3}}. \quad (5)$$

The other diagonal generator T_c^3 plays no role here because the degeneracy of color 1 and 2 ensures that there is no long range gluon 3-field. We take a constant rotated background U(1) magnetic field $\mathbf{B} = B\hat{z}$ along $+z$ axis. The gapped 2SC phase is \tilde{Q} -neutral, requiring a neutralizing background of strange quarks and/or electrons. The strange quark mass is assumed to be large enough at the moderate densities under consideration so that strange quarks do not play any dynamical role in the analysis.

III. THERMODYNAMIC POTENTIAL

The partition function in the presence of an external magnetic field B in the mean field approximation is given by

$$\mathcal{Z} = \mathcal{N} \int [d\bar{q}] [dq] \exp \left\{ \int_0^\beta d\tau \int d^3\vec{x} \left(\tilde{\mathcal{L}} - \frac{1}{2} B^2 \right) \right\}, \quad (6)$$

where \mathcal{N} is the normalization factor, $\beta = T^{-1}$ is the inverse of the temperature T , B is the external magnetic field and $\tilde{\mathcal{L}}$ is the Lagrangian density in terms of the rotated quantities. The full partition function \mathcal{Z} can be written as a product of three parts, $\mathcal{Z} = \mathcal{Z}_c \mathcal{Z}_{1,2} \mathcal{Z}_3$. Here, \mathcal{Z}_c serves as a constant multiplicative factor, $\mathcal{Z}_{1,2}$ denotes the contribution for quarks with color “1” and “2” and \mathcal{Z}_3 is for quarks with color “3”. These three parts can be expressed as

$$\mathcal{Z}_c = \mathcal{N} \exp \left\{ - \int_0^\beta d\tau \int d^3\vec{x} \left[\frac{\sigma^2}{4G_S} + \frac{\Delta^2}{4G_D} + \frac{B^2}{2} \right] \right\}, \quad (7)$$

$$\begin{aligned} \mathcal{Z}_{1,2} = \int [d\bar{Q}] [dQ] \exp \left\{ \int_0^\beta d\tau \int d^3\vec{x} \left[\frac{1}{2} \mathcal{L}_{\text{kin}}(Q, Q^c) \right. \right. \\ \left. \left. + \frac{1}{2} \tilde{e} \tilde{Q} (\bar{Q} \not{A} Q - \bar{Q}^c \not{A} Q^c) + \frac{1}{2} \bar{Q} \Delta^- Q^c + \frac{1}{2} \bar{Q}^c \Delta^+ Q \right] \right\}, \end{aligned} \quad (8)$$

$$\begin{aligned} \mathcal{Z}_3 = \int [d\bar{q}_3] [dq_3] \exp \left\{ \int_0^\beta d\tau \int d^3\vec{x} \left[\frac{1}{2} \mathcal{L}_{\text{kin}}(q_3, q_3^c) \right. \right. \\ \left. \left. + \frac{1}{2} \tilde{e} \tilde{Q} (\bar{q}_3 \not{A} q_3 - \bar{q}_3^c \not{A} q_3^c) \right] \right\}. \end{aligned} \quad (9)$$

The kinetic operators $\mathcal{L}_{\text{kin}}(q, q^c)$ now read $(i \not{\partial} + \mu \gamma^0 - M)$ where $M = m_0 + \sigma$ and we use the notation $\Delta^- (/ \Delta^+) = -i \gamma_5 \epsilon_f \epsilon_c \Delta (/ \Delta^*)$. In *flavor* \otimes *color* space in units of $\tilde{e} = \sqrt{3} g e / \sqrt{3 g^2 + e^2}$ the rotated charge matrix is given by $\tilde{Q} = Q \otimes \mathbf{1}_c - \mathbf{1}_f \otimes T^8 / 2\sqrt{3}$. Here, $\mathbf{1}_c$ and $\mathbf{1}_f$ are unit matrix on color and flavor spaces respectively. In our case, this translates to \tilde{Q} charges $u_{1,2} = 1/2, d_{1,2} = -1/2, u_3 = 1$ and $d_3 = 0$. With s -quarks as inert background, we also have $s_{1,2} = -1/2$ and $s_3 = 0$. Imposing the charge neutrality and β -equilibrium conditions is known to stress the pairing and lead to gluon condensation and a strong gluomagnetic field [52]. The role of such effects has been studied in [27], but here our focus is on the interdependence of the condensates and their response to the strong magnetic field.

Evaluation of the partition function and the thermodynamic potential, $\Omega = -T \ln \mathcal{Z} / V$ (where V is the volume of the system) is facilitated by introducing eight-component

Nambu-Gorkov spinors for each color and flavor of quark, leading to

$$\ln Z_{1,2} = \frac{1}{2} \ln \{\text{Det}(\beta G^{-1})\}; \quad \ln Z_3 = \frac{1}{2} \ln \{\text{Det}(\beta G_0^{-1})\}; \quad (10)$$

where G and G_0 are the quark propagators and inverse of the propagators are given by

$$G^{-1} = \begin{pmatrix} [G_{0,\tilde{Q}}^+]^{-1} & \Delta^- \\ \Delta^+ & [G_{0,-\tilde{Q}}^-]^{-1} \end{pmatrix}, \quad G_0^{-1} = \begin{pmatrix} [G_{0,\tilde{Q}}^+]^{-1} & 0 \\ 0 & [G_{0,-\tilde{Q}}^-]^{-1} \end{pmatrix}, \quad (11)$$

with $[G_{0,\tilde{Q}}^\pm]^{-1} = (\not{\partial} \pm \mu \gamma^0 + \tilde{e} \tilde{Q} \not{A} - m)$. The determinant computation is simplified by re-expressing the \tilde{Q} -charges in terms of charge projectors in the color-flavor basis, following techniques applied for the CFL phase [53]. The color-flavor structure of the condensates can be unraveled for the determinant computation by introducing energy projectors [8] and moving to momentum space, whereby we find

$$\begin{aligned} \ln Z_{1,2} &= \text{Tr}_{c,f} \sum_a \sum_{p_0, \mathbf{p}} [\ln(\beta^2(p_0^2 - (E_{\Delta,a}^+)^2) \beta^2(p_0^2 - (E_{\Delta,a}^-)^2))], \\ \ln Z_3 &= \text{Tr}_f \sum_a \sum_{p_0, \mathbf{p}} [\ln(\beta^2(p_0^2 - (E_{p,a}^+)^2) \beta^2(p_0^2 - (E_{p,a}^-)^2))], \end{aligned} \quad (12)$$

where $E_{\Delta,a}^\pm = \sqrt{(E_{p,a}^\pm)^2 + \Delta^2}$ with $E_{p,a}^\pm = E_{p,a} \pm \mu$ and $a = \{0, 1, \pm 1/2\}$. The energy $E_{p,a}$ is defined as $E_{p,a} = \sqrt{\mathbf{p}_{\perp,a}^2 + p_z^2 + m^2}$, if $a = 0$ then $\mathbf{p}_{\perp,0}^2 = p_x^2 + p_y^2$ else $\mathbf{p}_{\perp,a}^2 = 2|a|\tilde{e}Bn$. The sum over $p_0 = i\omega_k$ denotes the discrete sum over the Matsubara frequencies, n labels the Landau levels in the magnetic field which is taken in the \hat{z} direction.

IV. GAP EQUATIONS AND SOLUTION

Using the following identity we can perform the discrete summation over the Matsubara frequencies

$$\sum_{p_0} \ln[\beta^2(p_0^2 - E^2)] = \beta[E + 2T \ln(1 + e^{-\beta E})] \equiv \beta f(E). \quad (13)$$

Then we go over to the 3-momentum continuum using the replacement $\sum_{\mathbf{p}} \rightarrow V(2\pi)^{-3} \int d^3\mathbf{p}$, where V is the thermal volume of the system. Finally, the zero-field thermodynamic potential can be expressed as,

$$\Omega_{B=0} = \frac{\sigma^2}{4G_S} + \frac{\Delta^2}{4G_D} - 2 \int_0^\infty \frac{d^3\mathbf{p}}{(2\pi)^3} [f(E_p^+) + f(E_p^-) + 2f(E_\Delta^+) + 2f(E_\Delta^-)]. \quad (14)$$

In presence of a quantizing magnetic field, discrete Landau levels suggest the following replacement

$$\int_0^\infty \frac{d^3\mathbf{p}}{(2\pi)^3} \rightarrow \frac{|a|\tilde{e}B}{8\pi^2} \sum_{n=0}^\infty \alpha_n \int_{-\infty}^\infty dp_z, \quad (15)$$

where $\alpha_n = 2 - \delta_{n0}$ is the degeneracy factor of the n -th Landau level (all levels are doubly degenerate except the zeroth level). The thermodynamic potential in presence of magnetic field is given by

$$\begin{aligned} \Omega_{B \neq 0} = & \frac{\sigma^2}{4G_S} + \frac{\Delta^2}{4G_D} - \int_0^\infty \frac{d^3\mathbf{p}}{(2\pi)^3} [f(E_{p,0}^+) + f(E_{p,0}^-)] \\ & - \frac{\tilde{e}B}{8\pi^2} \sum_{n=0}^\infty \alpha_n \int_{-\infty}^\infty dp_z [f(E_{p,1}^+) + f(E_{p,1}^-) + 2f(E_{\Delta,\frac{1}{2}}^+) + 2f(E_{\Delta,\frac{1}{2}}^-)] . \end{aligned} \quad (16)$$

In either case, we can now solve the gap equations obtained by minimizing the (zero-temperature) thermodynamic potential Ω obtained in presence of magnetic field.

$$\text{Chiral gap equation : } \frac{\partial \Omega}{\partial m} = 0; \quad \text{Diquark gap equation : } \frac{\partial \Omega}{\partial \Delta} = 0. \quad (17)$$

Since the above equations involve integrals that diverge in the ultra-violet region, we must regularize in order to obtain physically meaningful results. We choose to regulate these functions using a sharp cut-off (step function in $|\mathbf{p}|$), which is common in effective theories such as the NJL model [39, 40], although one may also employ a smooth regulator [7, 53] without changing the results qualitatively for fields that are not too large². The momentum cut-off restrict the number of completely occupied Landau levels n_{max} which can be determined as follows

$$\int_0^\Lambda \frac{d^3\mathbf{p}}{(2\pi)^3} \rightarrow \frac{|a|\tilde{e}B}{8\pi^2} \sum_{n=0}^{n_{max}} \alpha_n \int_{-\Lambda'}^{\Lambda'} dp_z; \quad n_{max} = \text{Int} \left[\frac{\Lambda^2}{2|a|\tilde{e}B} \right]; \quad \Lambda' = \sqrt{\Lambda^2 - 2|a|\tilde{e}Bn}. \quad (18)$$

We use the fact that $p_z^2 \geq 0$ to compute n_{max} . For magnetic field $B \lesssim 0.02 \text{ GeV}^2$ ($\sim 10^{17} \text{ G}$, conversion to Gauss is given by $1 \text{ GeV}^2 = 5.13 \times 10^{19} \text{ G}$), n_{max} is of the order of 50 and the discrete summation over Landau levels becomes almost continuous. In that case, we recover the results of the zero magnetic field case as described in the next section. For fixed values of the free parameters, we were able to solve the chiral and

² For example, a smooth cutoff was employed in [53] to demonstrate the De-Haas Van Alphen oscillations in the gap parameter at very large magnetic field.

diquark gap equations self-consistently, for $B = 0$ as well as large B . Before discussing our numerical results, we note the origin of the interdependence of the condensates. The chiral gap equation contains only G_S which is determined by vacuum physics, but also depends indirectly on G_D/G_S (a free parameter) through Δ , which is itself dependent on the constituent $m = m_0 + \sigma$. Our numerical results can be understood as a consequence of this coupling and the fact that a large magnetic field stresses the $\bar{q}q$ pair (same \tilde{Q} charge, opposite spins implies anti-aligned magnetic moments) while strengthening the qq pair (opposite \tilde{Q} charge and opposite spins implies aligned magnetic moments).

V. NUMERICAL ANALYSIS

In order to investigate the competition between the chiral and the diquark condensates, in this section, we solve the two coupled gap equations (17) numerically. These gap equations involve integrals that have diverging behavior in the high-energy region (this is an artifact of the nonrenormalizable nature of the NJL model). Therefore, to obtain physically meaningful behavior, one has to regularize the diverging integrals by introducing some cutoff scale Λ . A sharp cutoff function sometimes leads to unphysical oscillations in thermodynamical quantities of interest, and especially for a system with discrete Landau levels. A novel regularization procedure called “Magnetic Field Independent Regularization” (MFIR) scheme [54, 55] can remove the unphysical oscillations completely even if a sharp cutoff function is used within MFIR. To reduce the unphysical behavior, it is very common in literature to use various smooth cutoff functions although they cannot completely remove the spurious oscillations. Here, we list a few of them:

- Fermi-Dirac type [56]: $f_c(p_a) = \frac{1}{2} \left[1 - \tanh \left(\frac{p_a - \Lambda}{\alpha} \right) \right]$ where α is a smoothness parameter.
- Woods-Saxon type [38]: $f_c(p_a) = \left[1 + \exp \left(\frac{p_a - \Lambda}{\alpha} \right) \right]^{-1}$ where α is a smoothness parameter.
- Lorentzian type [57]: $f_c(p_a) = \left[1 + \left(\frac{p_a^2}{\Lambda^2} \right)^N \right]^{-1}$ where N is a positive integer.

where $p_a = \sqrt{\mathbf{p}_{\perp,a}^2 + p_z^2}$, with $\mathbf{p}_{\perp,0}^2 = p_x^2 + p_y^2$ for $a = 0$ and $\mathbf{p}_{\perp,a}^2 = 2|a|\tilde{e}Bn$ for $a = 1, \pm 1/2$. Cutoff functions become smoother for larger values of α , or N in case of the Lorentzian

type of regulator. We have checked our numerical results for different cutoff schemes like sharp cutoff (Heaviside step function) and various smooth cutoff parameterizations as mentioned above and found that our main results are almost insensitive for different cutoff schemes. We therefore, use a smooth Fermi-Dirac type of regulator with $\alpha = 0.01\Lambda$ throughout numerical analysis.

One can fix various NJL model parameters – the bare quark mass m_0 , the momentum cutoff Λ and the scalar coupling constant G_S by fitting the pion properties in vacuum *viz.* the pion mass $m_\pi = 134.98$ MeV, the pion decay constant $f_\pi = 92.30$ MeV and the constituent quark mass $m(\mu = 0) = 0.33$ GeV. Similarly, one can fix the diquark coupling constant G_D by fitting the scalar diquark mass (~ 600 MeV) to obtain vacuum baryon mass of the order of ~ 900 MeV [58]. There are some factors that can, in principle, alter those model parameters *e.g.* strength of the external magnetic field, temperature, choice of the cutoff functions etc. Assuming that those factors have only small effects on the parameters and expecting that our numerical results would not change qualitatively, we fix the parameters in the isospin symmetric limit as follows (a discussion of the parameter choice can be found in Ref. [59])

$$m_{u,d} = m_0 = 5.5 \text{ MeV}, \quad \Lambda = 0.6533 \text{ GeV}, \quad G_S = 5.0163 \text{ GeV}^{-2}, \quad G_D = \rho G_S, \quad (19)$$

where ρ is a free parameter. Although Fierz transforming one gluon exchange implies $\rho = 0.75$ for $N_c = 3$ and fitting the vacuum baryon mass gives $\rho = 2.26/3$ [58], the underlying interaction at moderate density is bound to be more complicated, therefore we choose to vary the coupling strength of the diquark channel G_D to investigate the competition between the condensates.

We investigate the behavior of the chiral and diquark gaps along the chemical potential direction in presence of magnetic field for different magnitudes of the coupling ratio ρ ($= G_D/G_S$) at zero temperature. Before we discuss the influence of diquark gap on the chiral phase transition, we first demonstrate the behavior of the chiral gap for $\Delta = 0$ case (equivalently $\rho = 0$) for different magnitudes of $\tilde{e}B$. The choice of $\tilde{e}B$ is made to see the effects of the inclusion of different Landau levels in the system. In Table I, we show the values of n_1^{max} and $n_{\frac{1}{2}}^{max}$ and the corresponding values of the transition magnetic field $\tilde{e}B_t$. For example, if $\tilde{e}B < \tilde{e}B_t$, then the number of fully occupied Landau level, $n > n^{max}$. In Fig. 1, we show m as functions of μ in absence of diquark gap for different

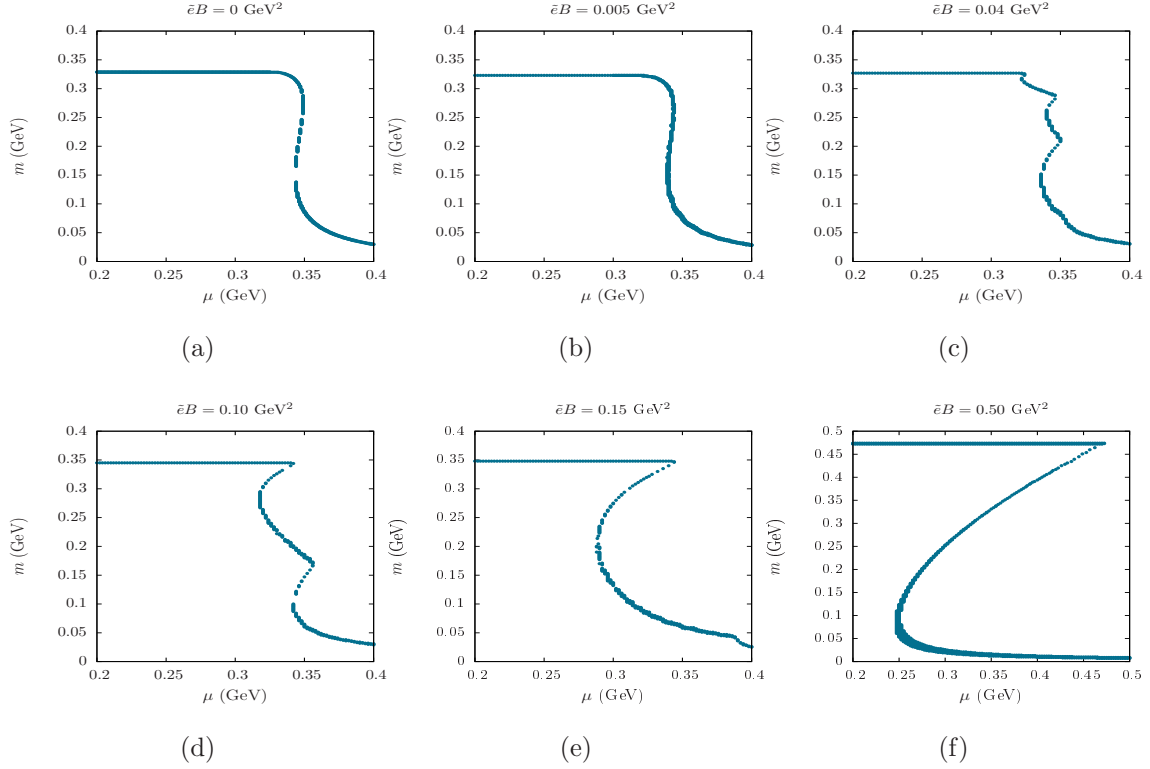


FIG. 1: Chiral gap m as functions of μ for $\rho = G_D/G_S = 0$ with increasing magnetic field $\tilde{e}B$ at $T = 0$.

choices of $\tilde{e}B$. In Figs. 1a and 1b, we show the m in absence of magnetic field ($\tilde{e}B = 0$) and in the weak magnetic field limit ($\tilde{e}B = 0.005 \text{ GeV}^2$ or equivalently $\sim 2.5 \times 10^{17} \text{ G}$) respectively. One can see that these two figures look almost identical. The reason is that the number of completely occupied Landau levels, n^{max} becomes very large (*e.g.* $n_1^{max} \sim 40$ for $\tilde{e}B \sim 0.005 \text{ GeV}^2$) in the weak magnetic field limit, making the discrete Landau level summation quasi-continuous. As we increase the magnetic field, noticeable deviations appear in the behavior of the chiral gap as seen in Figs. 1c to 1f.

From Fig. 1, it is clear that we get multiple solutions to the chiral gap equation for a small range of μ around the chiral phase transition region. For example, we get three solutions to the chiral gap equation for a narrow window of μ for zero or weak magnetic field ($\lesssim 2.5 \times 10^{17} \text{ G}$) cases. These three solutions correspond to the stable, metastable and unstable branches of the system. In Fig 2a, we plot the values of Ω corresponding to the three solutions obtained in the small μ -window. The value of the gap m for which

| $n_1^{max} =$ $\text{Int} \left[\frac{\Lambda^2}{2\tilde{e}B} \right]$ | $\tilde{e}B_t$ (GeV ²) | $n_{\frac{1}{2}}^{max} =$ $\text{Int} \left[\frac{\Lambda^2}{\tilde{e}B} \right]$ | $\tilde{e}B_t$ (GeV ²) |
|--|---------------------------------------|---|---------------------------------------|
| 1 | 0.213 | 1 | 0.427 |
| 2 | 0.107 | 2 | 0.213 |
| 3 | 0.071 | 3 | 0.142 |
| 4 | 0.053 | 4 | 0.107 |
| 5 | 0.043 | 5 | 0.085 |

TABLE I: The value of transition magnetic field $\tilde{e}B_t$ at successive numbers of fully occupied lowest Landau levels n_a^{max} where $a = 1, 1/2$ are the two possible values of the rotated charge \tilde{Q} .

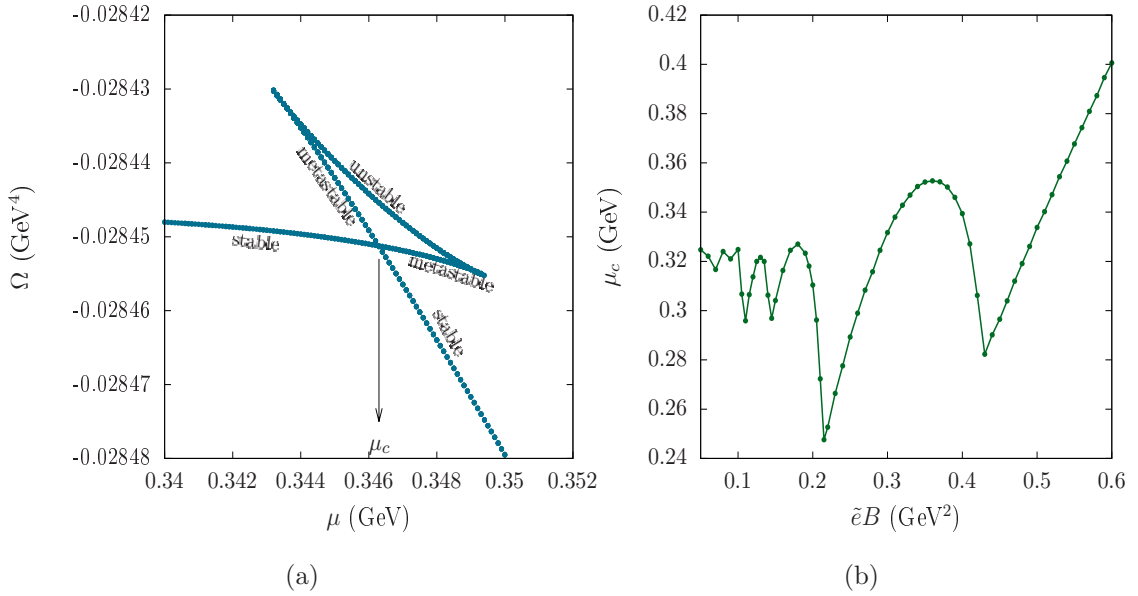


FIG. 2: (a) Thermodynamic potential (Ω) for $\Delta = 0$ and $\tilde{e}B = 0$ as a function of μ . The stable metastable and unstable branches of Ω are shown beside the curves. (b) The critical chemical potential for chiral phase transition (μ_c) for $\Delta = 0$ as a function of $\tilde{e}B$.

Ω is the lowest corresponds to the stable solution at any given density. The critical chemical potential μ_c (where the chiral and the diquark phase transitions occur) is the point where the first derivative of Ω (and the gaps) behave discontinuously. The location of μ_c gives the transition point from the stable region to the metastable region of the system. This can easily be identified by looking at the behavior of Ω as shown in Fig. 2a. We follow this method to locate the first order phase transition point. In Fig. 2b, we

plot μ_c as a function of $\tilde{e}B$. We observe that μ_c oscillates with $\tilde{e}B$ with dips whenever $\Lambda^2/(2|a|\tilde{e}B)$ takes an integer value, following the Shubnikov de Haas-van Alphen effect. Similar oscillations in the density of states and various thermodynamic quantities are observed in metals in presence of magnetic field at very low temperature. The magnitude of oscillations becomes more pronounced as we increase the magnetic field. If $\tilde{e}B \gtrsim 0.21 \text{ GeV}^2$ ($\sim 10^{19} \text{ G}$), only the zeroth Landau level is completely occupied as evident from Table I.

We observe multiple intermediate transitions (from Fig. 1c to Fig. 1d) due to the filling of successive Landau levels, and for a particular μ , sometimes there are two stable solutions at different densities for the same pressure. Similar multiple solutions of the gaps has been observed in the context of magnetized-NJL model with repulsive vector interactions [30]. Comparing the values of m at $\mu = 0$ for very strong magnetic field, one finds that m increases with $\tilde{e}B$. This is the magnetic catalysis effect [60–63]. It is also interesting to note that with increasing magnetic fields, the spread of the metastable region (the μ -window where we have multiple solutions) becomes wider. For example, the spread of the metastable regions for $\tilde{e}B = 0.5 \text{ GeV}^2$ is about 0.22 GeV and for $\tilde{e}B = 0.25 \text{ GeV}^2$ is about 0.12 GeV . These findings suggest the possibility of multiple phases with different values of dynamical mass in the presence of inhomogeneous magnetic fields, which we postpone to a future investigation. It is important to mention that the multiple solutions observed in chiral condensate as function of chemical potential would disappear when plotted as function of baryon density defined as $\langle \bar{q}\gamma^0 q \rangle$ (see e.g. Section 4.2 in Ref. [64]).

In Fig. 3, we show m and Δ as functions of μ for different ρ in presence of strong magnetic field. In [8], the competition of chiral and diquark gaps without any magnetic field was discussed in great detail. We observe that m increases with the increase of $\tilde{e}B$. For example, $m \sim 0.35 \text{ GeV}$ for $\tilde{e}B = 0.15 \text{ GeV}^2$ and $m \sim 0.48 \text{ GeV}$ for $\tilde{e}B = 0.5 \text{ GeV}^2$. In [8], it was shown that with the increase of ρ , the first order transition of the chiral and diquark gaps becomes crossover through a second-order phase transition. When a strong magnetic field is present, we find that the crossover becomes a first order transition. This is an important finding of this work, which has several implication for neutron star physics as discussed in the conclusion. The critical chemical potential μ_c is almost same for both the chiral and diquark phase transition, but takes on smaller values as we increase ρ for

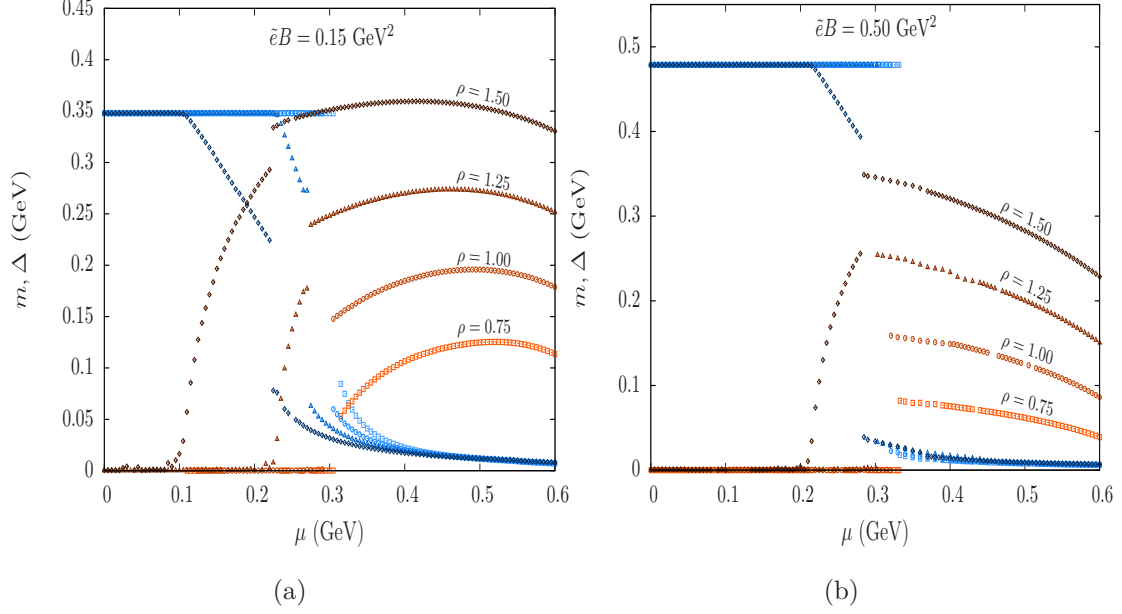


FIG. 3: The gaps m (different blue colors) and Δ (different brown colors) as functions of μ for different ρ in presence of strong magnetic field (a) $\tilde{e}B = 0.15 \text{ GeV}^2$ and (b) $\tilde{e}B = 0.50 \text{ GeV}^2$. The curves with square, circle, triangle and diamond represent $\rho = 0.75, 1, 1.25, 1.5$ respectively. The discontinuities in gaps signify a first-order phase transition.

a fixed $\tilde{e}B$ (as shown in Fig. 3).

In the weak (or zero) magnetic field limit, Δ appears at a smaller μ with increasing ρ and rises smoothly from zero, until it becomes discontinuous at μ_c . At μ_c , the chiral gap m also changes discontinuously, with the jumps in the gaps decreasing with increasing ρ . For instance, in Table II we see the jump in the chiral gap (δ_m) decreases from 0.250 GeV to 0.133 GeV as we increase ρ from 0.75 to 1.05. The corresponding jumps in diquark gap (δ_Δ) decreases from 0.077 GeV to 0.066 GeV. This picture does not change qualitatively until we go above a critical value $\rho = \rho_c \approx 1.09$. As long as $\rho < \rho_c$, the jumps in the gaps δ_m and δ_Δ remain nonzero but decrease as ρ moves towards ρ_c . In other words, the metastable region in Ω as shown in Fig. 2a shrinks with increasing ρ . At $\rho = \rho_c$ the metastable and unstable regions vanish completely. This qualifies it to be a second order phase transition. Above $\rho > \rho_c$, the gaps m and Δ are smoothly varying resulting in a smooth crossover. However, there always exists a pseudo-transition point (μ_c^p) around which fluctuations/variations of the condensates (*i.e.* derivatives of m and Δ w.r.t. μ) are sharply peaked. The width of these peaked distributions broaden with

| ρ | $\tilde{e}B = 0$ | | | | $\tilde{e}B = 0.1 \text{ GeV}^2$ | | | |
|--------|--------------------------|-------------------------------|-----------------------|--------------|----------------------------------|-------------------------------|-----------------------|-------------|
| | $\delta_m \text{ (GeV)}$ | $\delta_\Delta \text{ (GeV)}$ | $\mu_c \text{ (GeV)}$ | Nature | $\delta_m \text{ (GeV)}$ | $\delta_\Delta \text{ (GeV)}$ | $\mu_c \text{ (GeV)}$ | Nature |
| 0.75 | 0.250 | 0.077 | 0.332 | First order | 0.227 | 0.084 | 0.323 | First order |
| 1.05 | 0.133 | 0.063 | 0.295 | First order | 0.214 | 0.074 | 0.301 | First order |
| 1.09 | 0 | 0 | 0.289 | Second order | 0.198 | 0.066 | 0.297 | First order |
| 1.15 | Smooth | Smooth | 0.280 | Crossover | 0.185 | 0.051 | 0.295 | First order |
| 1.25 | Smooth | Smooth | 0.255 | Crossover | 0.122 | 0.038 | 0.284 | First order |

TABLE II: Critical chemical potential μ_c , jumps in the chiral (δ_m) and superconducting (δ_Δ) order parameters at μ_c for zero and $\tilde{e}B = 0.1 \text{ GeV}^2$ ($\sim 5 \times 10^{18} \text{ G}$) for various values of $\rho = G_D/G_S$. The nature of the transition is also indicated.

further increase of ρ , and μ_c^p moves to the left with increasing ρ . These results for $\tilde{e}B \approx 0$ agree qualitatively with the zero field results of [8] with minor quantitative differences at less than a few percent level. The region where the condensates coexist was termed by them as the “mixed broken phase”, since both chiral and (global) color symmetries are broken here. While it should not be confused with a genuine mixed phase, since the free energy admits a unique solution to the gap equations in this regime, it is clear that the width of this overlap region increases with increasing ρ .

The competition between the condensates is driven by the strong magnetic field, which in the case of m is a stress, since the chiral condensate involves quark spinors of opposite spin and same \tilde{Q} -charge. On the other hand, the diquark condensate, with opposite spin and \tilde{Q} -charge, is strengthened by the strong magnetic field. Thus, we expect a strengthening of the competition between the two condensates, resulting in a qualitative change from the zero-field case. With increasing ρ , similar to the $\tilde{e}B = 0$ case, δ_m and δ_Δ decrease and the transition is first order in nature. The dramatic effect we observe is that the mixed broken phase for large ρ at $\tilde{e}B = 0$ is no longer present in case of strong magnetic field case and the crossover region is replaced by a first-order transition. Specifically, in Table II, we see for $\rho = 1.25$, a smooth crossover in the $\tilde{e}B = 0$ case at $\mu_c^p \sim 0.255 \text{ GeV}$ becomes a first order transition with $\delta_m = 0.185 \text{ GeV}$ and $\delta_\Delta = 0.122 \text{ GeV}$ at $\mu_c \sim 0.284 \text{ GeV}$ for $\tilde{e}B = 0.1 \text{ GeV}^2$. The simultaneous appearance of the discontinuity in the gaps for large magnetic field case, at almost the same $\mu = \mu_c$ where

both the condensates have their most rapid variation in the $\tilde{e}B = 0$ case, is a physical feature and is also cutoff insensitive. We have checked that magnetic field $\tilde{e}B \lesssim 5 \times 10^{17}$ G does not notably alter the competition between the condensates from the zero magnetic field case.

VI. CONCLUSIONS

We study the effects of a strong homogeneous magnetic field on the chiral and diquark condensates in a two-flavor superconductor using the NJL model. We implement a self-consistent scheme to determine the condensates, by numerically iterating the coupled (integral) equations for the chiral and superconducting gaps. We obtain results for the nature of the competition between these condensates in two cases, at weak magnetic field limit where our results are qualitatively same as zero magnetic field results [8] and at strong magnetic field, where we find the competition between the gaps increases strongly causing a discontinuity in the gaps and disrupting the “mixed broken phase”. This is a result of the modified free energy of the quarks in the condensate when subjected to a strong magnetic field. For magnetic fields as large as $B \sim 10^{19}$ G, the anti-aligned magnetic moments of the quarks in the chiral condensate change the smooth crossover of the chiral transition to a sharp first order transition. The diquark gap also becomes discontinuous at this point. For magnetic fields $B \lesssim 10^{18}$ G, there is no significant effect of the magnetic field on the competition between the condensates and zero-field results apply.

These findings can impact the physics of hybrid stars (neutron stars with quark matter) or strange quark stars in several ways. Firstly, the structure of neutron stars is strongly affected by a first-order phase transition, with the possibility of a third family of compact stars in addition to neutron stars and white dwarfs [65] that is separated from conventional neutron stars by a radius gap of a few km. We can speculate that strange stars or hybrid stars with superconducting quark cores inside them belong to this third family. Since we find that a strong magnetic field increases the likelihood of a first-order phase transition and hence a mixed phase, magnetars could also possibly belong to this category of compact stars since they permit quark nucleation [66] and carry large interior magnetic fields which modify their mass-radius relationship [67]. Secondly, it was pointed out

in [27] that for large values of the local magnetic field and in the small density window of the metastable region, it is possible to realize domains or nuggets of superconducting regions with different values for the gap. Charge neutrality can also disrupt the mixed broken phase, but the oscillations of the chiral gap remain, leading to nucleation of chirally restored droplets. Such kinds of nucleation and domain formation will release latent heat that might be very large owing to the large value of the magnetic field, serving as an internal engine for possible energetic events on the surface of the neutron star [68, 69]. Such internal mechanisms are unlikely to occur in a pure neutron star without a quark core. Thirdly, strong magnetic fields and quark cores affect the radial and non-radial oscillation modes of neutron stars, which could be a discriminating feature in the gravitational wave signal from vibrating neutron stars. The frequency of the fundamental radial mode shows a kink at the density characterizing the onset of the mixed phase, and the frequencies depend on the magnetic field [70]. Non-radial modes such as g -modes can probe the density discontinuity arising as a result of the phase transition in neutron stars [71] or strange quark stars [72], although the effect of magnetic fields in this context is as yet unexplored. Another important aspect of rotating compact stars are the r -modes [73], which could be responsible for spinning down neutron stars or strange quark stars from their Kepler frequency down to the observed values seen in low-mass X-ray binaries. The effects of a strong magnetic field on the r -mode driven spin down of neutron stars have been studied in [74, 75], while r -modes in crystalline quark matter are discussed in [76]. The even-parity counterpart for the r -modes, which include non-radial oscillation modes such as the f - and p -modes have also been explored for the case of strange quark stars in [77, 78]. Our findings give additional motivation to the study of such interesting effects associated with a first-order transition in neutron stars with strong magnetic fields, and a systematic study of these effects in the new era of gravitational waves and neutron star observations may finally reveal the presence of quark matter in the core of neutron stars.

Acknowledgments

T.M. is supported by funding from the Carl Trygger Foundation under contract CTS-14:206 and the Swedish Research Council under contract 621-2011-5107. P.J. is supported

by the National Science Foundation under Grant No. PHY 1608959.

- [1] Bertrand C. Barrois. Superconducting Quark Matter. *Nucl. Phys.*, B129:390–396, 1977.
- [2] D. Bailin and A. Love. Superfluidity and Superconductivity in Relativistic Fermion Systems. *Phys. Rept.*, 107:325, 1984.
- [3] M. Iwasaki and T. Iwado. Superconductivity in the quark matter. *Phys. Lett.*, B350:163–168, 1995.
- [4] Mark G. Alford, Krishna Rajagopal, and Frank Wilczek. QCD at finite baryon density: Nucleon droplets and color superconductivity. *Phys. Lett.*, B422:247–256, 1998.
- [5] R. Rapp, Thomas Schfer, Edward V. Shuryak, and M. Velkovsky. Diquark Bose condensates in high density matter and instantons. *Phys. Rev. Lett.*, 81:53–56, 1998.
- [6] Mark G. Alford, Andreas Schmitt, Krishna Rajagopal, and Thomas Schfer. Color superconductivity in dense quark matter. *Rev. Mod. Phys.*, 80:1455–1515, 2008.
- [7] Mark G. Alford, Krishna Rajagopal, and Frank Wilczek. Color flavor locking and chiral symmetry breaking in high density QCD. *Nucl. Phys.*, B537:443–458, 1999.
- [8] Mei Huang, Peng-fei Zhuang, and Wei-qin Chao. Massive quark propagator and competition between chiral and diquark condensate. *Phys. Rev.*, D65:076012, 2002.
- [9] Amruta Mishra and Hiranmaya Mishra. Color superconducting 2SC+s quark matter and gapless modes at finite temperatures. *Phys. Rev.*, D71:074023, 2005.
- [10] Andrew W. Steiner, Sanjay Reddy, and Madappa Prakash. Color neutral superconducting quark matter. *Phys. Rev.*, D66:094007, 2002.
- [11] F. Neumann, M. Buballa, and M. Oertel. Mixed phases of color superconducting quark matter. *Nucl. Phys.*, A714:481–501, 2003.
- [12] Igor Shovkovy and Mei Huang. Gapless two flavor color superconductor. *Phys. Lett.*, B564:205, 2003.
- [13] Andreas Schmitt. *Spin-one color superconductivity in cold and dense quark matter*. PhD thesis, Frankfurt U., 2004.
- [14] Krishna Rajagopal and Rishi Sharma. The Crystallography of Three-Flavor Quark Matter. *Phys. Rev.*, D74:094019, 2006.
- [15] Charles Alcock, Edward Farhi, and Angela Olinto. Strange stars. *Astrophys. J.*, 310:261–

272, 1986.

- [16] Norman K. Glendenning, S. Pei, and F. Weber. Signal of quark deconfinement in the timing structure of pulsar spindown. *Phys. Rev. Lett.*, 79:1603–1606, 1997.
- [17] Dany Page and Vladimir V. Usov. Thermal evolution and light curves of young bare strange stars. *Phys. Rev. Lett.*, 89:131101, 2002.
- [18] Prashanth Jaikumar, Madappa Prakash, and Thomas Schfer. Neutrino emission from Goldstone modes in dense quark matter. *Phys. Rev.*, D66:063003, 2002.
- [19] Sanjay Reddy, Mariusz Sadzikowski, and Motoi Tachibana. Neutrino rates in color flavor locked quark matter. *Nucl. Phys.*, A714:337–351, 2003.
- [20] Prashanth Jaikumar, Craig D. Roberts, and Armen Sedrakian. Direct Urca neutrino rate in colour superconducting quark matter. *Phys. Rev.*, C73:042801, 2006.
- [21] J. Berdermann, D. Blaschke, T. Fischer, and A. Kachanovich. Neutrino emissivities and bulk viscosity in neutral two-flavor quark matter. *Phys. Rev.*, D94(12):123010, 2016.
- [22] Prashanth Jaikumar, Gautam Rupak, and Andrew W. Steiner. Viscous damping of r-mode oscillations in compact stars with quark matter. *Phys. Rev.*, D78:123007, 2008.
- [23] Dmitri E. Kharzeev, Larry D. McLerran, and Harmen J. Warringa. The Effects of topological charge change in heavy ion collisions: 'Event by event P and CP violation'. *Nucl. Phys.*, A803:227–253, 2008.
- [24] V. Skokov, A. Yu. Illarionov, and V. Toneev. Estimate of the magnetic field strength in heavy-ion collisions. *Int. J. Mod. Phys.*, A24:5925–5932, 2009.
- [25] V. Voronyuk, V. D. Toneev, W. Cassing, E. L. Bratkovskaya, V. P. Konchakovski, and S. A. Voloshin. (Electro-)Magnetic field evolution in relativistic heavy-ion collisions. *Phys. Rev.*, C83:054911, 2011.
- [26] Bohdan Paczynski. GB 790305 as a very strongly magnetized neutron star. *Acta Astron.*, 42:145–153, 1992.
- [27] Tanumoy Mandal and Prashanth Jaikumar. Neutrality of a magnetized two-flavor quark superconductor. *Phys. Rev.*, C87:045208, 2013.
- [28] Pablo G. Allen and Norberto N. Scoccola. Quark matter under strong magnetic fields in SU(2) NJL-type models: parameter dependence of the cold dense matter phase diagram. *Phys. Rev.*, D88:094005, 2013.
- [29] Monika Sinha, Xu-Guang Huang, and Armen Sedrakian. Strange quark matter in strong

- magnetic fields within a confining model. *Phys. Rev.*, D88(2):025008, 2013.
- [30] Robson Z. Denke and Marcus Benghi Pinto. Influence of a repulsive vector coupling in magnetized quark matter. *Phys. Rev.*, D88(5):056008, 2013.
 - [31] A. G. Grunfeld, D. P. Menezes, M. B. Pinto, and N. N. Scoccola. Phase structure of cold magnetized quark matter within the SU(3) NJL model. *Phys. Rev.*, D90(4):044024, 2014.
 - [32] Debarati Chatterjee, Thomas Elghozi, Jerome Novak, and Micaela Oertel. Consistent neutron star models with magnetic field dependent equations of state. *Mon. Not. Roy. Astron. Soc.*, 447:3785, 2015.
 - [33] Pablo G. Allen, Valeria P. Pagura, and Norberto N. Scoccola. Cold magnetized quark matter phase diagram within a generalized SU(2) NJL model. *Phys. Rev.*, D91(11):114024, 2015.
 - [34] Robson Z. Denke and Marcus Benghi Pinto. Coexistence of Multiple Phases in Magnetized Quark Matter with Vector Repulsion. 2015.
 - [35] Tanumoy Mandal and Prashanth Jaikumar. Effect of temperature and magnetic field on two-flavor superconducting quark matter. *Phys. Rev.*, D94(7):074016, 2016.
 - [36] Mark Alford and Krishna Rajagopal. Absence of two flavor color superconductivity in compact stars. *JHEP*, 06:031, 2002.
 - [37] D. N. Aguilera, D. Blaschke, and H. Grigorian. How robust is a 2SC quark matter phase under compact star constraints? *Nucl. Phys.*, A757:527–542, 2005.
 - [38] Sh. Fayazbakhsh and N. Sadooghi. Color neutral 2SC phase of cold and dense quark matter in the presence of constant magnetic fields. *Phys. Rev.*, D82:045010, 2010.
 - [39] T. M. Schwarz, S. P. Klevansky, and G. Papp. The Phase diagram and bulk thermodynamical quantities in the NJL model at finite temperature and density. *Phys. Rev.*, C60:055205, 1999.
 - [40] M. Buballa and M. Oertel. Color flavor unlocking and phase diagram with selfconsistently determined strange quark masses. *Nucl. Phys.*, A703:770–784, 2002.
 - [41] Amruta Mishra and Hiranmaya Mishra. Chiral symmetry breaking, color superconductivity and color neutral quark matter: A Variational approach. *Phys. Rev.*, D69:014014, 2004.
 - [42] Juergen Berges and Krishna Rajagopal. Color superconductivity and chiral symmetry restoration at nonzero baryon density and temperature. *Nucl. Phys.*, B538:215–232, 1999.
 - [43] Gregory W. Carter and Dmitri Diakonov. Chiral symmetry breaking and color supercon-

- ductivity in the instanton picture. In *Understanding deconfinement in QCD: Proceedings, International Workshop, Trento, Italy, 1-13 Mar 1999*, 1999.
- [44] Benoit Vanderheyden and A. D. Jackson. A Random matrix model for color superconductivity at zero chemical potential. *Phys. Rev.*, D61:076004, 2000.
 - [45] Huan Chen, Wei Yuan, Lei Chang, Yu-Xin Liu, Thomas Klahn, and Craig D. Roberts. Chemical potential and the gap equation. *Phys. Rev.*, D78:116015, 2008.
 - [46] M. Bocquet, S. Bonazzola, E. Gourgoulhon, and J. Novak. Rotating neutron star models with magnetic field. *Astron. Astrophys.*, 301:757, 1995.
 - [47] A. E. Broderick, M. Prakash, and J. M. Lattimer. Effects of strong magnetic fields in strange baryonic matter. *Phys. Lett.*, B531:167–174, 2002.
 - [48] Mark G. Alford, Juergen Berges, and Krishna Rajagopal. Magnetic fields within color superconducting neutron star cores. *Nucl. Phys.*, B571:269–284, 2000.
 - [49] T. Klahn, D. Blaschke, F. Sandin, C. Fuchs, A. Faessler, H. Grigorian, G. Ropke, and J. Trumper. Modern compact star observations and the quark matter equation of state. *Phys. Lett.*, B654:170–176, 2007.
 - [50] Luca Bonanno and Armen Sedrakian. Composition and stability of hybrid stars with hyperons and quark color-superconductivity. *Astron. Astrophys.*, 539:A16, 2012.
 - [51] Jens O. Andersen and Lars Kyllingstad. Pion Condensation in a two-flavor NJL model: the role of charge neutrality. *J. Phys.*, G37:015003, 2009.
 - [52] Efraim J. Ferrer and Vivian de la Incera. Magnetic fields boosted by gluon vortices in color superconductivity. *Phys. Rev. Lett.*, 97:122301, 2006.
 - [53] Jorge L. Noronha and Igor A. Shovkovy. Color-flavor locked superconductor in a magnetic field. *Phys. Rev.*, D76:105030, 2007. [Erratum: *Phys. Rev.* D86,049901(2012)].
 - [54] D. P. Menezes, M. Benghi Pinto, S. S. Avancini, A. Perez Martinez, and C. Providencia. Quark matter under strong magnetic fields in the Nambu-Jona-Lasinio Model. *Phys. Rev.*, C79:035807, 2009.
 - [55] Pablo G. Allen, Ana G. Grunfeld, and Norberto N. Scoccola. Magnetized color superconducting cold quark matter within the $SU(2)_f$ NJL model: A novel regularization scheme. *Phys. Rev.*, D92(7):074041, 2015.
 - [56] Kenji Fukushima and Harmen J. Warringa. Color superconducting matter in a magnetic field. *Phys. Rev. Lett.*, 100:032007, 2008.

- [57] Marco Frasca and Marco Ruggieri. Magnetic Susceptibility of the Quark Condensate and Polarization from Chiral Models. *Phys. Rev.*, D83:094024, 2011.
- [58] D. Ebert, L. Kaschluhn, and G. Kastelewicz. Effective meson - diquark Lagrangian and mass formulas from the Nambu-Jona-Lasinio model. *Phys. Lett.*, B264:420–425, 1991.
- [59] Michael Buballa. NJL model analysis of quark matter at large density. *Phys. Rept.*, 407:205–376, 2005.
- [60] K. G. Klimenko. Three-dimensional Gross-Neveu model in an external magnetic field. *Theor. Math. Phys.*, 89:1161–1168, 1992. [Teor. Mat. Fiz.89,211(1991)].
- [61] K. G. Klimenko. Three-dimensional Gross-Neveu model at nonzero temperature and in an external magnetic field. *Z. Phys.*, C54:323–330, 1992.
- [62] V. P. Gusynin, V. A. Miransky, and I. A. Shovkovy. Catalysis of dynamical flavor symmetry breaking by a magnetic field in (2+1)-dimensions. *Phys. Rev. Lett.*, 73:3499–3502, 1994. [Erratum: Phys. Rev. Lett.76,1005(1996)].
- [63] V. P. Gusynin, V. A. Miransky, and I. A. Shovkovy. Dimensional reduction and dynamical chiral symmetry breaking by a magnetic field in (3+1)-dimensions. *Phys. Lett.*, B349:477–483, 1995.
- [64] Thomas Michael Schwarz. *Thermodynamics of the chiral condensate*. Dissertation, Technische Universitt Mnchen, Mnchen, 2003.
- [65] A. Ayriyan, D. E. Alvarez-Castillo, D. Blaschke, and H. Grigorian. Mass-radius constraints for the neutron star EoS - Bayesian analysis. *J. Phys. Conf. Ser.*, 668(1):012038, 2016.
- [66] D. Kroff and E. S. Fraga. Nucleating quark droplets in the core of magnetars. *Phys. Rev.*, D91(2):025017, 2015.
- [67] M. Orsaria, Ignacio F. Ranea-Sandoval, and H. Vucetich. Magnetars as Highly Magnetized Quark Stars: an analytical treatment. *Astrophys. J.*, 734:41, 2011.
- [68] J. L. Zdunik, M. Bejger, P. Haensel, and E. Gourgoulhon. Strong first-order phase transition in a rotating neutron star core and the associated energy release. *Astron. Astrophys.*, 479:515, 2008.
- [69] Ritam Mallick and P. K. Sahu. Phase transitions in neutron star and magnetars and their connection with high energetic bursts in astrophysics. *Nucl. Phys.*, A921:96–113, 2014.
- [70] R. Panda, K. K. Mohanta, and K. Sahu. Radial modes of oscillations of slowly rotating magnetized compact hybrid stars. *J. Phys. Conf. Ser.*, 599(1):012036, 2015.

- [71] G. Miniutti, J. A. Pons, E. Berti, L. Gualtieri, and V. Ferrari. Non-radial oscillation modes as a probe of density discontinuities in neutron stars. *Mon. Not. Roy. Astron. Soc.*, 338:389, 2003.
- [72] Hajime Sotani, Kazuhiro Tominaga, and Kei-ichi Maeda. Density discontinuity of a neutron star and gravitational waves. *Phys. Rev.*, D65:024010, 2002.
- [73] Nils Andersson. A New class of unstable modes of rotating relativistic stars. *Astrophys. J.*, 502:708–713, 1998.
- [74] Xu-Guang Huang, Mei Huang, Dirk H. Rischke, and Armen Sedrakian. Anisotropic Hydrodynamics, Bulk Viscosities and R-Modes of Strange Quark Stars with Strong Magnetic Fields. *Phys. Rev.*, D81:045015, 2010.
- [75] Jan E. Staff, Prashanth Jaikumar, Vincent Chan, and Rachid Ouyed. Spindown of Isolated Neutron Stars: Gravitational Waves or Magnetic Braking? *Astrophys. J.*, 751:24, 2012.
- [76] Bettina Knippel and Armen Sedrakian. Gravitational radiation from crystalline color-superconducting hybrid stars. *Phys. Rev.*, D79:083007, 2009.
- [77] Hajime Sotani and Tomohiro Harada. Nonradial oscillations of quark stars. *Phys. Rev.*, D68:024019, 2003.
- [78] C. V. Flores and G. Lugones. Discriminating hadronic and quark stars through gravitational waves of fluid pulsation modes. *Class. Quant. Grav.*, 31:155002, 2014.